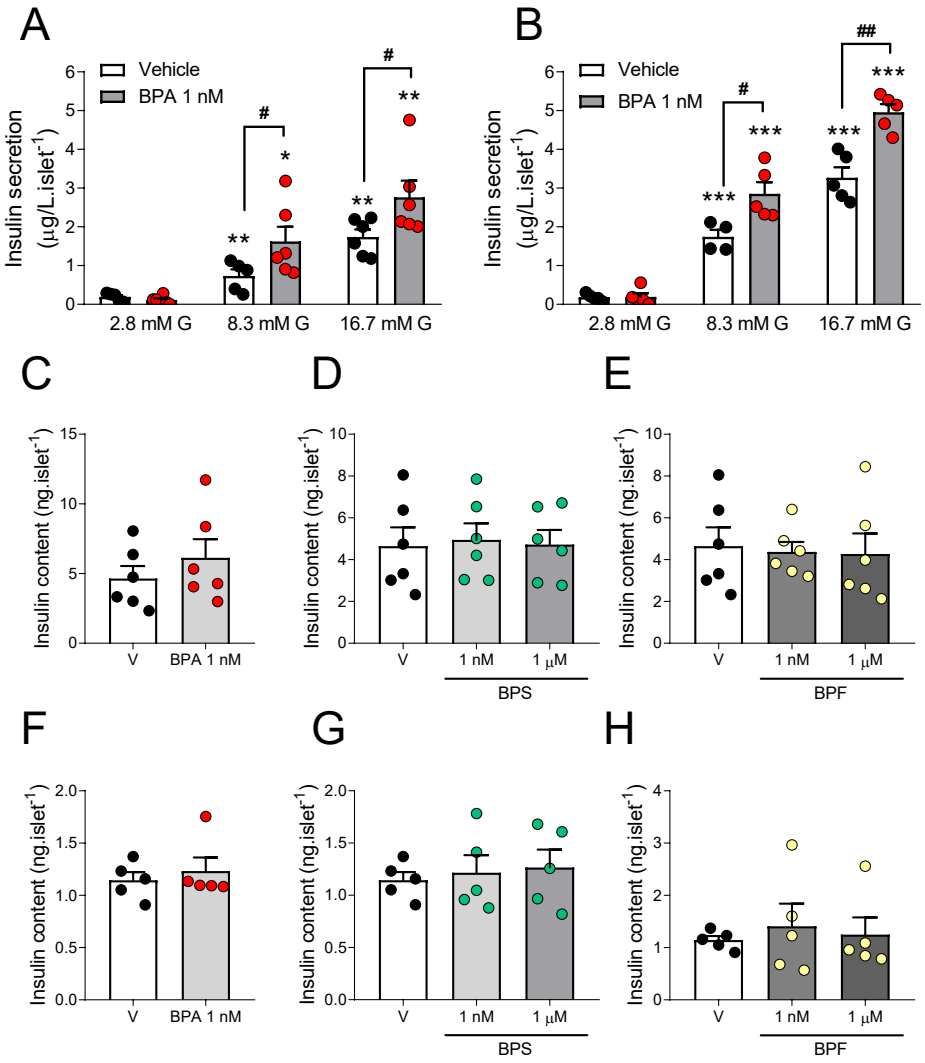

Figure S1. Insulin secretion and content upon treatment with bisphenols. **(A and B)** Insulin secretion was measured at 2.8, 8.3 and 16.7 mM glucose in islets from C57BL/6J mice treated *ex vivo* with vehicle (control; black circles and white bars) or 1 nM BPA (red circles and light grey bars). **(A)** After 2 h of recovery, treatments (vehicle or BPA) were added to each glucose solution so that the islets remained under treatment during the whole experiment. **(B)** Islets were treated *ex vivo* with vehicle or BPA for 48 h, and then, glucose-stimulated insulin secretion was performed in the absence of treatments. **(C-H)** Insulin content was measured after GSIS of the experiments described in the **Figure 1**. Mouse islets from C57BL/6J mice treated *ex vivo* with vehicle (control; black circles and white bars), 1 nM BPA (**A and F**; red circles), BPS (**D and G**; green circles) or BPF (**E and H**; yellow circles). Insulin content was measured by ELISA. Data are shown as means ± SEM of six independent islet preparations isolated on three different days: *p≤0.05, **p≤0.01, ***p≤0.001 vs 2.8 mM; $^{\#}$p≤0.05, $^{\#\#}$p≤0.01, $^{\#\#\#}$p≤0.001 comparisons indicated by bars (one-way ANOVA); $^{\&}$p≤0.05 (Student's t-test).

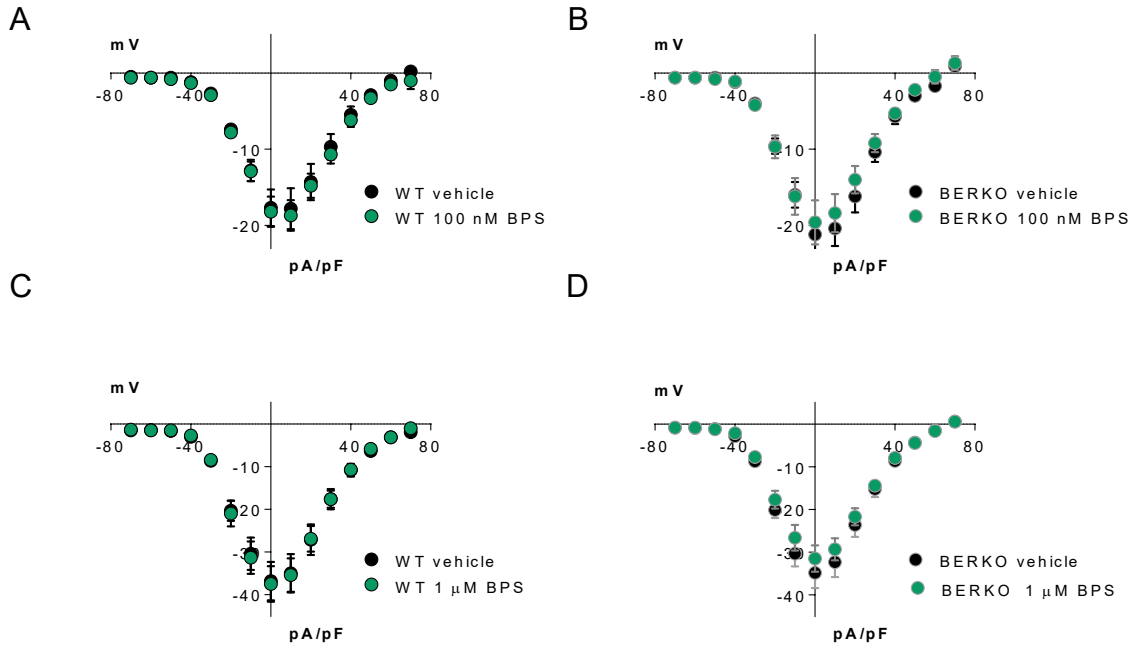

Figure S2. 100 nM and 1µM BPS do not reduce whole-cell Ca^{2+} currents ~~via ERβ~~ in *β-cells*. (**A and B)** Average relationship between Ca^{2+} current density (Ca^{2+} currents in pA normalized to the cell capacitance in pF) and the voltage of the pulses in wild-type (WT, **A and C**) and BERKO (**B and D**) control cells (black circles) and cells treated (green circles) with 100 nM BPS (**A** and **B**) or 1 µM BPS (**C and D**). The effect of BPS was measured after 48 h of incubation. The methodology for patch-clamp recordings of voltage-gated Ca^{2+} currents is the same as the one described in Figure 4. Data are shown as means ± SEM of the number of cells recorded in WT (n=10-15 cells) and BERKO (n=7-15 cells) mice. These cells were isolated from six mice on at least three different days: *p≤0.05 vs control (one-way ANOVA).

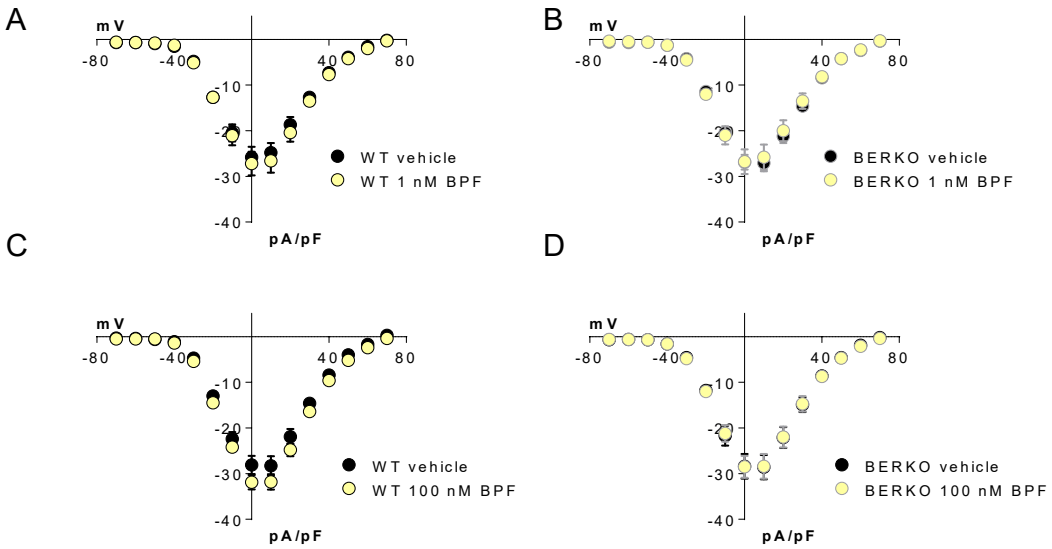

Figure S3. 1 nM and 100 nM of BPF do not reduce whole-cell Ca^{2+} currents ~~via ERβ~~ in *β-cells*. (**A and B)** Average relationship between Ca^{2+} current density (Ca^{2+} currents in pA normalized to the cell capacitance in pF) and the voltage of the pulses in wild-type (WT, **A and C**) and BERKO (**B and D**) control cells (black circles) and cells treated (yellow circles) with 1 nM BPF (**A and B**) or 100 nM BPF (**C and D**). The effect of BPF was measured after 48 h of incubation. The methodology for patch-clamp recordings of voltage-gated Ca^{2+} currents is the same as the one described in Figure 4. Data are shown as means ± SEM of the number of cells recorded in WT (n=13-21 cells) and BERKO (n=9-23cells) mice. These cells were isolated from six mice on at least three different days: *$p \leq 0.05$ vs control (one-way ANOVA).

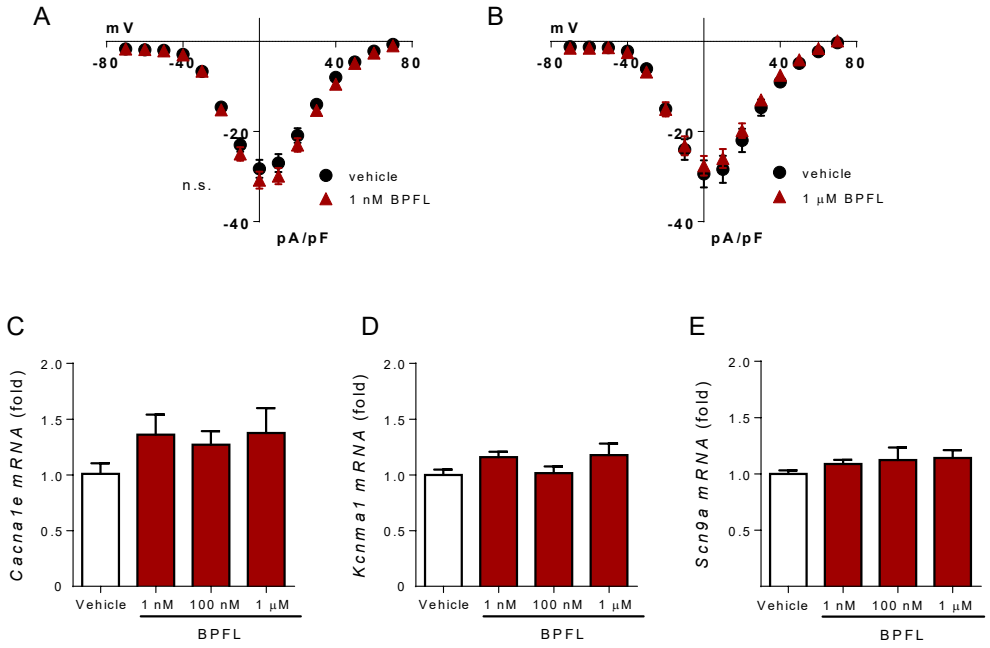

Figure S4. Bisphenol FL does not change whole-cell Ca^{2+} currents or *Cacna1e*, *Kcnma1* and *Scn9a* mRNA expression in mouse islets. (**A and B**) Average relationship between Ca^{2+} current density (Ca^{2+} currents in pA normalized to the cell capacitance in pF) and the voltage of the pulses (-60 to +70 mv from a holding potential of -70 mV, 50 ms duration) in isolated β-cells treated *in vitro* with vehicle (black circles) or with 1 nM BPFL (**A**; red triangles) or 1 µM BPFL (**B;** red triangles). The effect of BPFL was measured after 48 h of incubation. Data are shown as means ± SEM of the number of cells recorded in vehicle (n=8-10 cells) and BPFL (n=7-9 cells). These cells were isolated from six mice on at least three different days (**C-E**) mRNA expression of *Cacna1e* **(C)**, *Kcnma1* **(D)** and *Scn9a* **(E)** was measured in islets from C57BL/6J mice treated *ex vivo* with vehicle (white bars) or BPFL (red bars) at 1 nM, 100 nM, and 1 µM for 48 h. mRNA expression was measured by qRT-PCR and normalized to the housekeeping gene *Hprt1,* and is shown as fold vs. mean of the controls. Data are shown as means ± SEM of: four to twenty independent samples from up to twenty islets preparations isolated on at least three different days (one-way ANOVA).

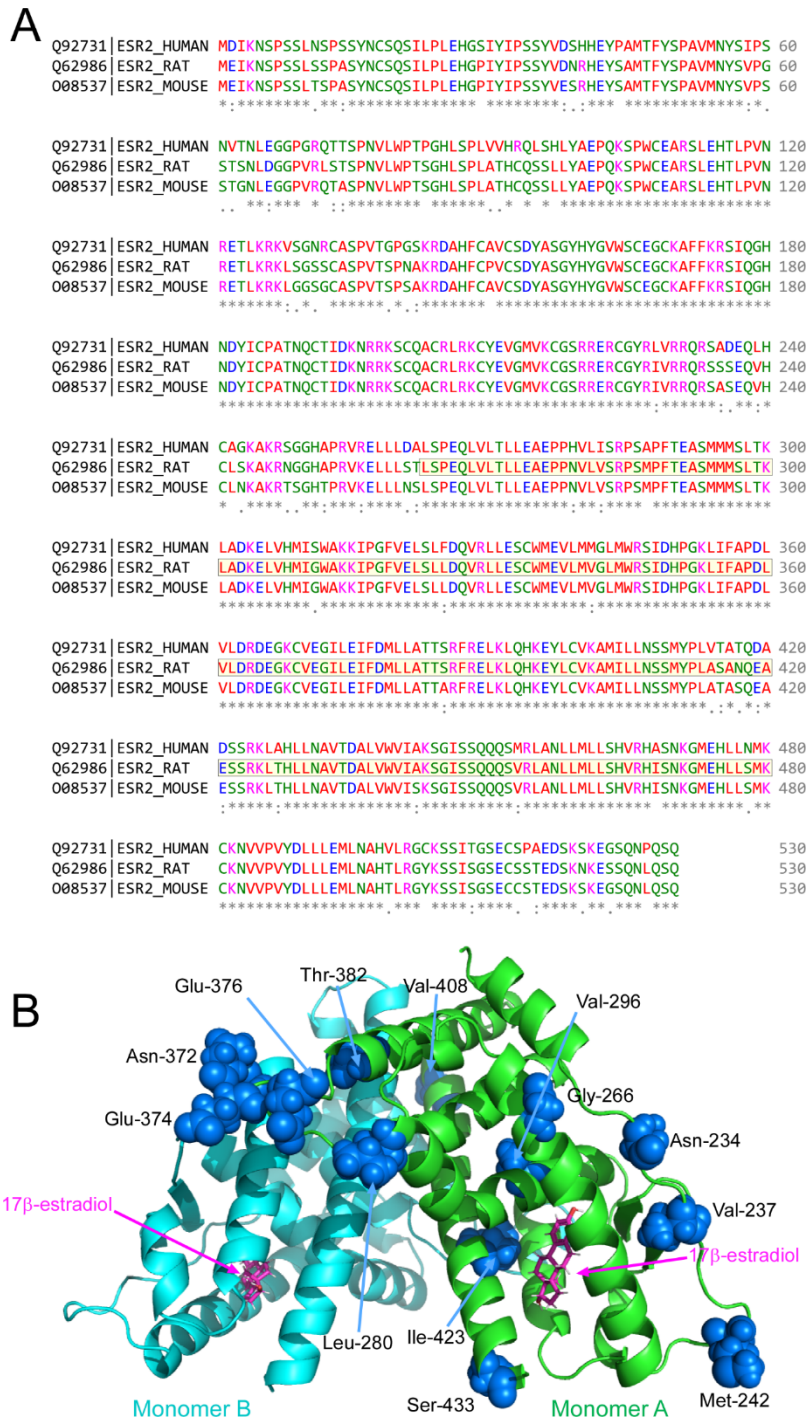

Figure S5. Sequence alignment of human, rat and mouse LBD-ERβ. (**A**) Multiple sequence alignment of human, rat and mouse ERβ. A yellow box indicates the region of the protein corresponding to the LBD and whose structure has been resolved from x-ray diffraction data. An orange box locates the human Cys-339 that can be palmitoylated. (**B**) Secondary structure of the rat ERβ-LBD dimer (PDB ID 1HJ1) that includes a 17β-estradiol molecule in the ligand-binding cavity of each subunit. Monomer A (green) highlights the different amino acids (spheres, Asn-234, Val-237, Met-242, Gly-266, Leu-280, Val-296, Ala-369, Ser-370, Asn-372, Glu-374, Glu-376, Thr-382, Val-408, Ile-423, Ser-433) in the human isoform.

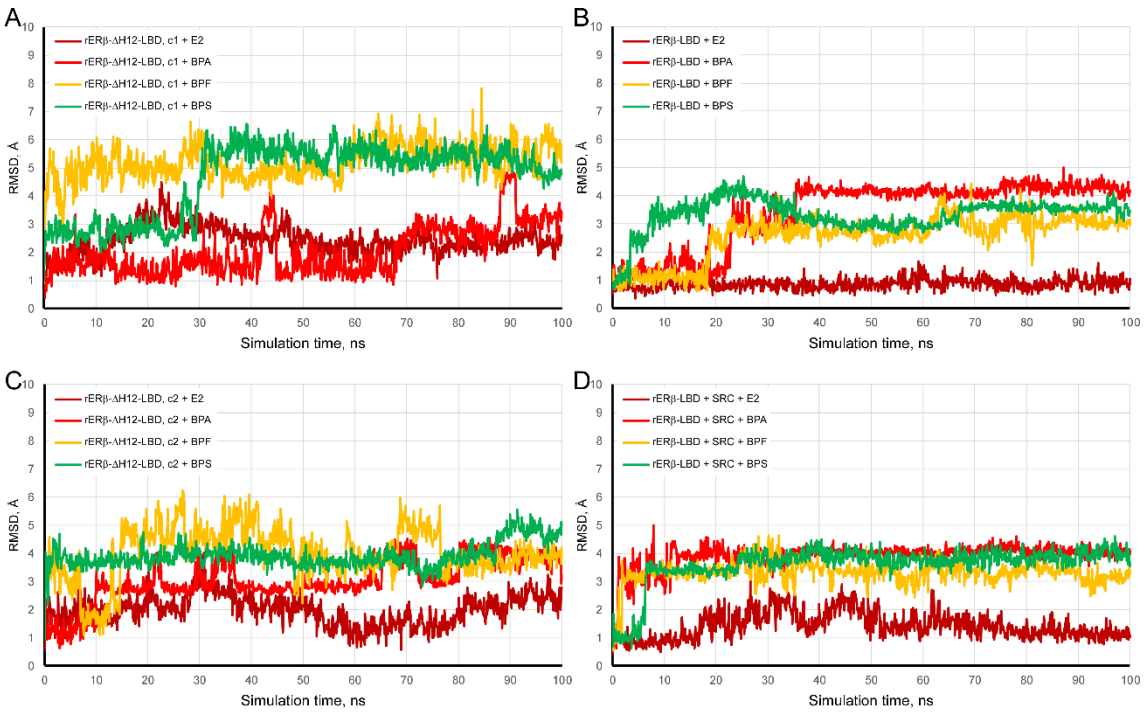

Figure S6. Analysis of trajectories for molecular dynamics simulations of LBD-ER in complex with different ligands. A and C Trajectories (RMSD, Å) of the different ligands initially docked to the main cavity of the open rERβ-ΔH12-LBD dimer. Cavity 1 (c1, **A**) and cavity 2 (c2, **C**). **B** and **D** Trajectories (RMSD, Å) of the different ligands docked to the closed cavity of the rERβ-LBD monomer in the absence **(B)** or presence **(D)** of the SRC co-activating peptide, respectively. The legends included within each panel indicate the different ligands analyzed.

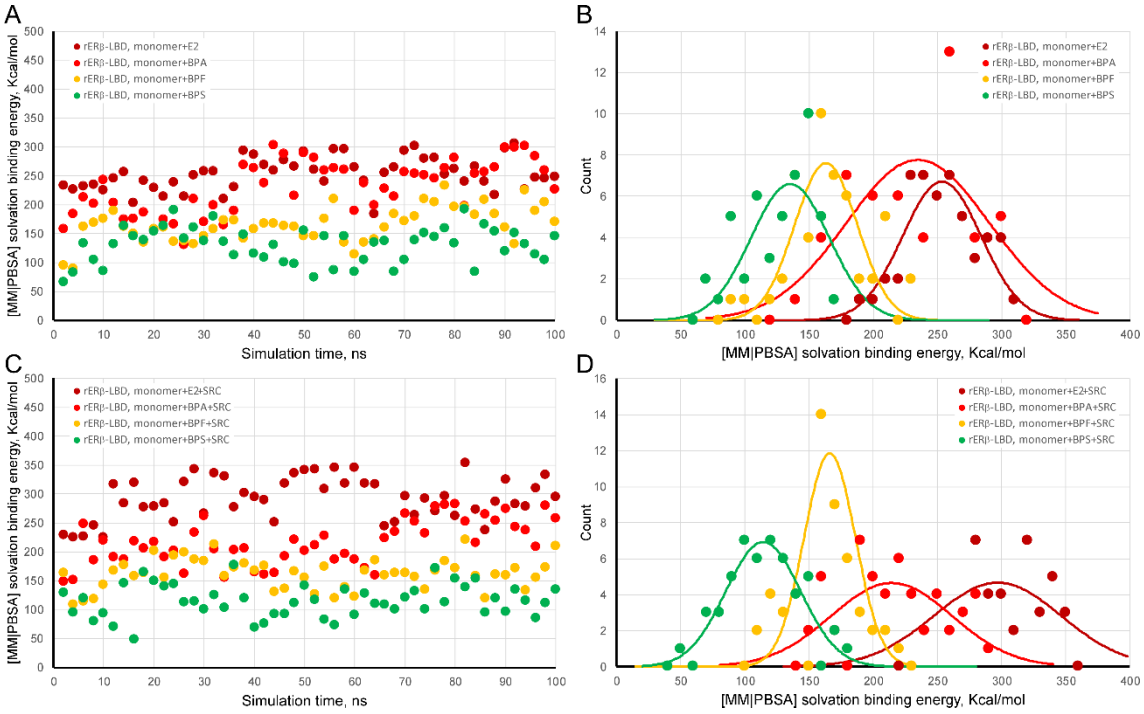

Figure S7. Calculated MM/PBSA solvation binding energy for bound E2 and bisphenols to the H12 closed rERβ-LBD alone or in the presence of the Src peptide. (A and C) Calculated MM/PBSA solvation binding energy values of each ligand attached to LBD cavity alone **(A)** or in the presence of the Src peptide **(C)**. **(B and D)** Frequency distributions of the values shown in **(A)** and **(C)**, respectively. A Gaussian curve overlaps discrete data. The legends included within each panel indicate the different ligands analyzed.